Biostatistics (2002), **3**, 4, *pp.* 493–510
Printed in Great Britain

A stochastic model for extinction and recurrence of epidemics: estimation and inference for measles outbreaks

BÄRBEL F. FINKENSTÄDT*
Department of Statistics, University of Warwick, Coventry, CV4 7AL, UK and Department of Zoology, University of Cambridge, Cambridge, CB2 3EJ, UK
stsbe@csv.warwick.ac.uk

OTTAR N. BJØRNSTAD
Department of Entomology, Penn State University, PA 16802, USA

BRYAN T. GRENFELL
Department of Zoology, University of Cambridge, Cambridge, CB2 3EJ, UK

SUMMARY

Epidemic dynamics pose a great challenge to stochastic modelling because chance events are major determinants of the size and the timing of the outbreak. Reintroduction of the disease through contact with infected individuals from other areas is an important latent stochastic variable. In this study we model these stochastic processes to explain extinction and recurrence of epidemics observed in measles. We develop estimating functions for such a model and apply the methodology to temporal case counts of measles in 60 cities in England and Wales. In order to estimate the unobserved spatial contact process we suggest a method based on stochastic simulation and marginal densities. The estimation results show that it is possible to consider a unified model for the UK cities where the parameters depend on the city size. Stochastic realizations from the dynamic model realistically capture the transitions from an endemic cyclic pattern in large populations to irregular epidemic outbreaks in small human host populations.

Keywords: Discrete latent variable; Population dynamics; Stochastic modelling of infectious diseases; Stochastic simulation; Time series of counts.

1. INTRODUCTION

Infectious diseases are a major cause of misery, sickness and death in humans and animals worldwide. Control and prevention is therefore an important task both from a humane and an economic point of view. Efficient intervention hinges on a complete understanding of disease transmission and persistence. Dynamic modelling of infectious diseases has contributed greatly to this end (Anderson & May, 1991). From a dynamic point of view, infectious diseases can be divided in two main classes, those that are *endemic*, i.e. locally persistent within their host populations, and those that are not. Many sexually transmitted diseases exemplify the former, while influenza exemplifies the latter. Non-endemic, that is *epidemic* diseases are introduced into the host population, break out, and burn out locally. Such diseases can only persist through recurrent epidemics (Bartlett, 1956). Since chance events are major

*To whom correspondence should be addressed

determinants of the size and the timing of the outbreak, epidemic dynamics pose a great challenge to stochastic modelling. Reintroduction of the disease through contact with infected individuals from other areas is an important stochastic variable, as is the time to extinction. The low counts of infected individuals towards the beginning and the end of outbreaks further imply that demographic stochasticity is important.

In terms of nonlinear dynamics the particular focus has been on childhood infections resulting in a distinguished history of deterministic (Soper, 1929; Kermack & McKendrick, 1933; London & Yorke, 1973; Dietz, 1975, 1976; Schenzle, 1984; Anderson & May, 1991) and stochastic (Bartlett, 1956, 1957, 1960a,b) modelling of disease dynamics. A recent development is to unify these dynamical models and nonlinear time series analysis. Initially, this work used nonparametric methods to search for chaos and other nonlinear phenomena in time series of notified cases (Schaffer & Kot, 1985; Olsen & Schaffer, 1990; Sugihara *et al.*, 1990; Ellner, 1991; Nychka *et al.*, 1992; Grenfell, 1992; Tidd *et al.*, 1993; Ellner & Turchin, 1995). More recently, semi-mechanistic (Ellner *et al.*, 1998) and mechanistic approaches (Finkenstädt & Grenfell, 2000) have been used to confront dynamical models with time series data. Bobashev *et al.* (1998) present a promising approach to uncovering the unknown dynamics of the individuals that are susceptible to measles. They demonstrate that the susceptible data reconstructed by their method improve the forecasting of notified measles cases if included as a covariate in a non-parametric autoregressive modelling approach. Thus far all these examine the dynamics of measles and other diseases in large endemic host populations.

In this study we present a model for these stochastic processes, extending the approach developed in Finkenstädt & Grenfell (2000) to cover both *epidemic* and *endemic* dynamics. The disease transmission is modelled as a discrete SIR (susceptible–infected–recovered) model comprising the infected and susceptible classes as state variables. Our aim is to develop a model that can capture epidemic as well as endemic dynamics and the transition between these regimes. Secondly, we present an estimating approach for this model. We apply the methodology to case counts of measles—a childhood disease that is observed to exhibit both kinds of dynamics depending on the host community size. This study was motivated by measles in cities in England and Wales prior to immunization programmes. Our assumptions are empirically justified for measles but should also be applicable to other diseases with a natural history that pertains to an SIR model, notably infectious childhood diseases with permanent immunity.

In his now classic work Bartlett (1957, 1960a) estimated a critical community size (CCS) of about 250 000 to 300 000 inhabitants for measles. The CCS is the population size large enough to maintain transmission in epidemic troughs. Large cities, above the CCS, exhibit endemic dynamics. Centres below the CCS exhibit series of epidemic outbreaks interrupted by extinction (Grenfell, 1992; Rhodes *et al.*, 1997).

We first give some necessary background on the dynamics of childhood diseases focusing in particular on measles. We use this to develop a stochastic time series model and an approach to estimate its parameters. The estimation is complicated by the presence of unobserved and partially observed state variables as well as state dependent variances. We assess consistency of estimators in finite samples through a Monte Carlo study. In order to make inferences about the unobserved spatial contact we use stochastic simulation and marginal densities. The estimation results indicate that it is possible to consider a unified epidemic model where the parameters are predicted from simple functions of the population size. We illustrate that the estimated dynamic model realistically captures the transition from an endemic cyclic pattern to regular and irregular epidemic outbreaks.

2. PERSISTENCE AND EXTINCTION OF EPIDEMICS

At the heart of epidemics lies the often nonlinear transmission of the disease from infected and infectious individuals—called *infecteds* for short—to susceptible individuals, here called *susceptibles*

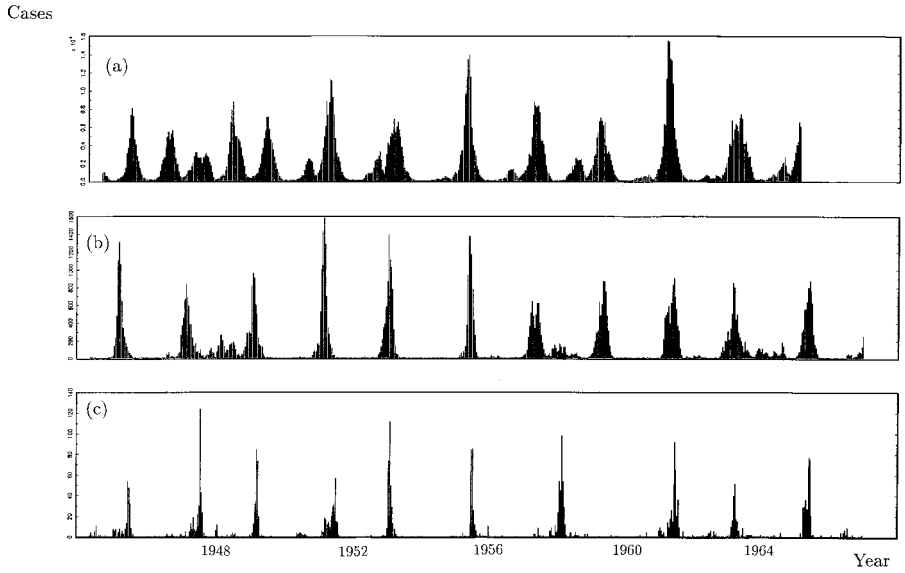

Fig. 1. Time series plots of reported cases corrected for temporal under-reporting for (a) London (3.3 million inhabitants), (b) Plymouth (210 000 inhabitants), (c) Teignmouth (10 000 inhabitants) during the pre-vaccination time from 1944 to 1966. The population sizes stated in brackets are the approximate median yearly sizes for this time period.

(Anderson & May, 1991). For childhood infections such as measles this transmission rate is subject to strong seasonal variation over the school year since both the infected and susceptible populations largely comprise schoolchildren (Fine & Clarkson, 1982; Schenzle, 1984). The latent and infectious period, of around two weeks, is followed by lifelong immunity in measles. Measles epidemics are in this sense self-limiting. The depletion of susceptibles can only be counteracted by susceptible replenishment through births.

We focus on weekly measles notifications in 60 towns and cities in England and Wales. These are official notifications, taken from the Registrar General's Weekly Reports—more details of the data set are given in Keeling & Grenfell (1997), Grenfell & Harwood (1997) and Grenfell & Bolker (1998). The clearest epidemic dynamics are before the onset of measles vaccination in 1967. We therefore analyse the pre-vaccination data set from the start of 1944 to the end of 1966. Local annual birth rates and population sizes are taken from the Annual Reports of the Registrar General.

Before the UK mass vaccination programme the disease dynamics led to a pattern of biennial epidemics with alternating years of minor and major disease incidence. Figure 1 illustrates the observed time pattern of pre-vaccination measles incidence for three cities in England and Wales from large to small population sizes. During times of higher birth rates, the accelerated replenishment into the susceptible class gave rise to annual cycles (Finkenstädt & Grenfell, 2000). This is observed at the time of the baby boom around 1947 as well as on the individual city level for places characterized by permanent high birth rates such as Liverpool (Finkenstädt *et al.*, 1998). The regular cyclicity of endemic populations, i.e. cities large enough to maintain a chain of transmission in epidemic troughs, was classified as type I dynamics by Bartlett (1957). The observed pattern for London in Figure 1(a) provides an example of such regular type I dynamics.

The pattern becomes qualitatively different for smaller populations where susceptibles become

depleted to the extent that the chain of transmission is interrupted. The time series indicate frequent extinction of the disease (zero incidence) after major outbreaks. However, intermediate-sized communities exhibit regular recurrence of the disease in synchrony with the epidemics in large communities. Bartlett (1957) coined this type II dynamics. The case reports for Plymouth in Figure 1(b) provide an example of such dynamics. Small communities, such as Teignmouth (shown in Figure 1(c)), are characterized by pronounced periods of extinction and sporadic recurrence of the disease, classified by Bartlett as type III.

In most cities in England and Wales, therefore, the incidence is driven partly by extinction and reintroduction of the disease. In this study we seek to develop an appropriate stochastic formulation and a statistical framework for inference that can be applied to data on this type of outbreak.

The pattern of local extinction is determined by three factors: (a) the size and recruitment into the susceptible class given by birth rates, (b) the rate of contact by local susceptibles with infecteds from other populations and (c) the rate of contact of susceptible and infected individuals within the community. This is subject to seasonal variation due to social heterogeneities of individuals and the aggregation of schoolchildren as modulated by the schooling/holiday pattern (Fine & Clarkson, 1982). Several studies (Yorke & London, 1973; London & Yorke, 1973; Dietz, 1975; Schwartz, 1985) have shown that the seasonal variation in transmissibility is very important as it is capable of producing longer-term oscillations in the dynamics of epidemics. For simplicity we refer to point (b) as either *migration* or *influx of infection* and to the schooling pattern in point (c) as *seasonal forcing*.

3. STOCHASTIC MODEL

Let $Y_t \geqslant 0$ denote the true number of infecteds in a host population at time t. This is a non-negative random variable with discrete probability distribution P_y and expectation λ_t at time t. Let y_t denote a realization from Y_t. Furthermore, let $\Theta_t \geqslant 0$ denote a random variable for the influx of infection with discrete probability distribution P_θ and let θ_t be a realization of Θ_t. As in generalized linear modelling we assume that the disease intensity λ_t is determined by a set of stimulus variables through a predictor function, where here the function is dictated by the theory of disease dynamics. The elementary model is based on a discrete deterministic model developed by Fine & Clarkson (1982), as extended to include migration of infecteds and to allow for linear or nonlinear incidence rates (see also Lui *et al.* (1987)).

For measles, the characteristic time scale of the disease, i.e. the duration of the transition from infection to recovery and lifelong immunity, is two weeks (Black, 1984). Therefore any new infection in biweek t must arise from an interaction between the same individual as a susceptible and another infected individual sometime within the previous biweek. If we therefore aggregate the data into two-weekly time steps then the future number of infecteds can be explained as a function of the previous number of infecteds. The appropriate discrete-dynamic two-dimensional compartment model for a childhood disease that entails lifelong immunity is thus given by

$$E(Y_t|y_{t-1}, \theta_{t-1}, S_{t-1}) = \lambda_t = r_t(y_{t-1} + \theta_{t-1})^{\alpha_1} S_{t-1}^{\alpha_2} \tag{1}$$

$$Y_t \sim P_y(\lambda_t) \tag{2}$$

$$\theta_t \sim P_\theta(\theta) \tag{3}$$

$$S_t = B_t + S_{t-1} - y_t. \tag{4}$$

Here S_t is the number or density of susceptibles, B_t denotes the number of births, and r_t is a factor of proportionality or transmission parameter that varies seasonally through the school year. Furthermore, α_1 and α_2 denote mixing parameters. In standard models $\alpha_1 = \alpha_2 = 1$, i.e. the incidence rate is bilinear, being proportional to the density of susceptibles and infectives. This corresponds to the assumption that the contact process between susceptible and infected individuals is governed through homogeneous mixing or by 'mass action'. Equations (1)–(4) represent a fully specified probability model for an epidemic

process. We are interested in estimating the seasonal transmission parameters r_t, the mixing parameters α_1, α_2, and the mean influx of infection θ. It is worth emphasizing some important features. Firstly, the model is doubly stochastic in the sense that both the influx of infecteds, Θ_t, as well as the transmission process, Y_t, are random processes. Both are discrete and non-negative implying that the model is non-Gaussian. Secondly, the model is nonlinear because of the disease transmission (1) between infecteds and susceptibles. In particular, the stochastic influx process enters the stochastic epidemic process in a nonlinear fashion.

The model possesses the following fundamental properties. If the number of susceptible individuals is positive, i.e. $S_{t-1} > 0$, the following cases can be distinguished:

- If there are no contacts with infectious migrants, the number of infecteds depends only on the past local infecteds since $y_{t-1} > 0 \Longrightarrow \lambda_t > 0$.
- When the disease has faded out, it remains so for as long as there is no contact with an infected migrant, i.e. $\theta_{t-1} = 0$ and $y_{t-1} = 0 \Longrightarrow \lambda_t = 0$. This holds true irrespective of any other quantities in the system. Therefore a sequence of realizations of zero infecteds does not reveal information about the transmission and mixing parameters.
- The disease can only be reintroduced after extinction if there is contact with infecteds from other host populations. This follows from $\lambda_t > 0 \Longleftrightarrow$ either $\theta_{t-1} > 0$ or $y_{t-1} > 0$.

If there are no susceptibles the disease goes extinct, since $S_{t-1} = 0 \Longrightarrow \lambda_t = 0$. This also holds true irrespective of any other quantities in the system.

One major complication in estimating such a model arises from the fact that the migration of infecteds θ_t is an unobserved stochastic process in time. The observed variables of the system are the local births and the reported number of cases where the latter are under-reported. Finkenstädt & Grenfell (2000) describe in detail how it is possible to reconstruct the dynamics of the susceptible class S_t as deviation from its time-invariant average $\overline{S}$ using time series data on locally reported cases and births. The reconstruction is based on (4) and provides a variable Z_t with mean zero so that $S_t = Z_t + \overline{S}$. The mean density of susceptibles $\overline{S}$ is unknown. The deviations from the mean, Z_t, follow the same dynamics as S_t in (4). Susceptible reconstruction has the additional benefit of revealing the temporal rate of under-reporting. This rate can be interpreted as a factor that accounts for the balance between the births entering the susceptible class and the infecteds leaving it. The notified cases can hence be corrected for under-reporting. For the purpose of this study, we focus attention on estimating the parameters of the transmission equation (1) for which we make the following assumptions:

(A1) The sequence of reconstructed susceptibles Z_t can be treated as a fixed covariate in (1). The mean number of susceptibles $\bar{S}$ is constant in time. Furthermore, Y_t can be approximated by the notified cases corrected for under-reporting.

(A2) Influx Θ_t is a discrete nonnegative stochastic process with constant mean $\theta \in \mathbf{R}_+^0$. Let $\delta_t = \theta_t - \theta$ denote the deviation from the mean influx and let $\mu_r = E(\delta_t^r)$ denote the rth central moment (assumed to exist as needed).

(A3) The influx Θ_t and the number of infecteds Y_t are independent random variables at each time point t.

(A4) The contact rate r_t is a time varying parameter with period one year $r_t = r_{t \bmod s}$ where s is the number of observations per year, i.e. $s = 26$ for biweekly data.

4. Estimation

The epidemic process in (1)–(4) is defined by a set of observed (y_t, B_t), partially observed (S_t) and unobserved (θ_t) variables. Estimation and inference thus requires a sequence of steps using the assumptions stated above.

Using assumption (A1) we write the conditional expectation in (1) as

$$\lambda_t = r_t(y_{t-1} + \theta_{t-1})^{\alpha_1}(Z_{t-1} + \overline{S})^{\alpha_2}. \tag{5}$$

Noting that the epidemic time contains all information about the mixing and transmission parameters we apply the logarithmic transformation to the non-zero subset of the data i.e. the subset of data for which $y_{t-1} + \theta_{t-1} > 0$, hence

$$\log \lambda_t = \log r_t + \alpha_1 \log(y_{t-1} + \theta_{t-1}) + \alpha_2 \log(Z_{t-1} + \overline{S}). \tag{6}$$

Since $\bar{S}$ is unobserved we approximate $\log(Z_{t-1} + \overline{S})$ in (6) by

$$\log(Z_{t-1} + \overline{S}) \approx \log \overline{S} + \frac{Z_{t-1}}{\overline{S}}. \tag{7}$$

We checked that the first-order approximation works well for simulated data from an epidemic model (see Finkenstädt & Grenfell (2000)). The transmission equation in (6) hence becomes

$$\log \lambda_t = \log r_t^* + \zeta Z_{t-1} + \alpha_1 \log(y_{t-1} + \theta_{t-1}), \tag{8}$$

where $r_t^* = r_t \bar{S}^{\alpha_2}$, and $\zeta = \alpha_2/\bar{S}$. Since the mean susceptible density $\bar{S}$ is unknown, the mixing parameter α_2 and the transmission parameters r_t cannot be identified. However, they are identifiable as functions of $\bar{S}$. r_t^* is the infection rate of one infected individual introduced into a population with $\bar{S}$ susceptibles. We expect the average infection rate r_t^* to be approximately constant for different sizes of the host population whereas ζ should be decreasing with population size.

The next step is to approximate the term $\log(y_{t-1}+\theta_{t-1})$ in the transmission equation (8) to account for the unobserved θ_{t-1}. The question of how well the term $\log(y_{t-1} + \theta_{t-1})$ can be approximated around the observed y_{t-1} depends on the size of y_{t-1} relative to θ_{t-1}. For an endemic community the influx is small in comparison to the local number of infecteds. Hence, $\log(y_{t-1} + \theta_{t-1})$ may simply be approximated by $\log(y_{t-1})$. However, typically for an epidemic community a very small number of infecteds is observed prior to and after extinction such that y_{t-1} and θ_{t-1} may temporarily be of similar size. We therefore should consider a higher-order approximation. The question of how high an order will be addressed in a Monte Carlo study below.

Considering an approximation of up to order three, and writing $\theta_t = \theta + \delta_t$ (assumption (A2)), we have

$$\log(y_{t-1} + \theta_{t-1}) \approx \log y_{t-1} + \frac{\theta + \delta_{t-1}}{y_{t-1}} - \frac{1}{2}\left(\frac{\theta + \delta_{t-1}}{y_{t-1}}\right)^2 + \frac{1}{3}\left(\frac{\theta + \delta_{t-1}}{y_{t-1}}\right)^3 + \cdots. \tag{9}$$

Using assumption (A3) the components in (9) can be separated into the conditional mean of y_t given y_{t-1} and a remainder e_t with mean zero,

$$\log(y_{t-1} + \theta_{t-1}) = \log y_{t-1} + c_1 y_{t-1}^{-1} + c_2 y_{t-1}^{-2} + c_3 y_{t-1}^{-3} + e_t, \tag{10}$$

where $c_1 = \theta$, $c_2 = -(\theta^2 + \mu_2)/2$, $c_3 = (\theta^3 + \mu_3 + 3\theta\mu_2)/3$ are the coefficients of the Taylor expansion and μ_k stands for the kth central moment of the influx process (A2). Note that the expansion coefficients are functions of the parameters of the influx process. Each additional expansion term involves moments of higher order of the influx process which are weighted inversely by polynomials in the immediate past number of infecteds. The importance of the migratory influx is thus larger for small populations and during the time of epidemic troughs.

Incorporating (7), and considering an expansion up to order three for the influx process (10), the full transmission equation in (8) is thus approximated by

$$\log y_t = \log r_t^* + \zeta Z_{t-1} + \alpha_1 \log y_{t-1} + \alpha_1(c_1 y_{t-1}^{-1} + c_2 y_{t-1}^{-2} + c_3 y_{t-1}^{-3}) + \varepsilon_t, \tag{11}$$

which we will refer to as the full model. The error process of the full model is

$$\varepsilon_t = \frac{y_t - \lambda_t}{\lambda_t} + \alpha_1 e_t, \tag{12}$$

with expectation zero and variance function

$$V(\varepsilon_t) = \frac{V(y_t)}{\lambda_t^2} + \alpha_1^2 V(e_t). \tag{13}$$

Since the model is doubly stochastic, the variance function (13) of the full model accounts for the two sources of variation. The first term contains the variance as in an ordinary generalized linear model (see McCullagh and Nelder (1997, chapter 2)) where $V(y_t)$ is the variance of the stochastic epidemic process and is determined by the probability distribution P_y. The second term contains the variation due to the unobserved stochastic influx process.

Finally, the full model in (11) can be reformulated as a regression model that is linear in the parameter vector β,

$$\log y_t = x_t \beta + \varepsilon_t. \tag{14}$$

Here, $x_t = (D_t, Z_{t-1}, \log y_{t-1}, y_{t-1}^{-1}, y_{t-1}^{-2}, y_{t-1}^{-3}) \in \mathbf{R}^{5+s}$ denotes the vector of covariates where $D_t = (D_{1,t}, \ldots, D_{s,t})$ is an s-dimensional vector of dummies with $D_{i,t} = 1$ if $t = i \bmod s$ and $D_{i,t} = 0$ otherwise. The parameter vector is $\beta = (\log r^*_{t \bmod s}, \zeta, \alpha_1, \alpha_1 c_1, \alpha_1 c_2, \alpha_1 c_3)'$ where $\log r^*_{t \bmod s}$ is a vector of $s = 26$ seasonal parameters. Note that the last three elements of β are associated with the approximation of the influx process. Equation (14) represents a generalized linear model with nonlinear variance function given in (13). For $E(\varepsilon_t) = 0$ and since $E(x_t \varepsilon_t) = 0$ the OLS estimator $\hat{\beta}_{\mathrm{LS}}$ is consistent. Note that the condition for consistency $E(\varepsilon_t) = 0$ depends on whether the approximation of the influx process (9) is of sufficient order. The heteroscedastic error term, however, implies that the weighted LS estimator

$$\hat{\beta}_{\mathrm{WLS}} = \left(\sum_{t=1}^{T} \frac{x_t x_t'}{V(\varepsilon_t)} \right)^{-1} \sum_{t=1}^{T} \frac{x_t \log y_t}{V(\varepsilon_t)} \tag{15}$$

is of smaller variation than the ordinary LS estimator. Since $V(\varepsilon_t)$ depends on unknown parameters and on the influx process we use estimated WLS where $V(\varepsilon_t)$ is replaced by an estimate. The approximate variance function of the influx process is a complex polynomial function of y_{t-1} the estimation of which is complicated by the fact that (a) estimating a polynomial variance function from residuals generally produces an error term with nonzero expectation, and (b) extrapolating from estimated polynomials does not always yield positive variances in numerical applications. Different solutions to this are possible. In order to use a simpler weighting scheme that is robust in numerical applications we assume that $V(\varepsilon_t)$ can be modelled as an exponential function of the predicted values (see Harvey (1976)),

$$V(\varepsilon_t) = \exp(\gamma_0 + \gamma_1 \log \lambda_t). \tag{16}$$

This variance function encompasses the variance of the stochastic epidemic process (first term of (13), but the parameters (γ_0, γ_1) can adjust to account for additional dispersion due to the stochastic influx.

5. MONTE CARLO STUDY OF LS ESTIMATORS

We next assess the finite-sample performance of $\hat{\beta}_{\mathrm{LS}}$ and $\hat{\beta}_{\mathrm{WLS}}$ in a simulation study of the stochastic epidemic model (1)–(4) for assumed parameter values. In particular, we want to know (a) if WLS gains efficiency although it is based on a simplified variance function and (b) how consistency is affected by the degree of approximation in (9).

5.1 *Simulation model and parameters*

We simulate time series from the doubly stochastic model for six different sizes of host populations: 22 000, 60 000, 160 000, 440 000, 1.2 million and 3.3 million inhabitants. This approximately corresponds to the range of community sizes in the 60-cities data set. In order to obtain realistic parameter values for the simulation study, we used $\hat{\beta}_{\mathrm{LS}}$ from the London data for $c_1 = c_2 = c_3 = 0$, i.e. neglecting the influx. We then simulate time series from the stochastic model given in (1)–(4), standardized by the mean susceptible density $\bar{S}$, i.e. we replace (1) by $r_t^*(y_{t-1}+\theta_{t-1})^{\alpha_1} \exp(\zeta Z_{t-1})$, and (4) by $Z_t = B_t + Z_{t-1} - y_t$.

To simulate the behaviour for the different community sizes we use the London estimates for the mixing parameter α_1, which was estimated to be 0.975, and for the set of seasonal transmission rates r_t^*. The parameter that requires adjustment to different community sizes is $\zeta = \alpha_2/\bar{S}$ which was estimated to be 8.93×10^{-6} for London. Assuming $\alpha_2 = 1$, the mean number of susceptibles $\bar{S}$ is around 112 000 which corresponds to 3% of the London population size. Following this rule, we adapted ζ to any other community sizes. The birth rate was set as 17 per thousand inhabitants per year which corresponds to the observed mean birth rate. The mean influx was set as $\theta = \exp(-3)$ per biweek for all community sizes. Finally, following Kendall (1949), we assume that P_y in (2) is a negative binomial distribution with dispersion parameter $(y_{t-1} + \theta_{t-1})$, and P_θ is a Poisson distribution with intensity θ. Allowing for a transient of 400 iterations the estimators β_{LS} and β_{WLS} are computed from 100 time series simulations of length $T = 600$. This corresponds approximately to the sampling time of $T = 572$ for the real data.

5.2 *Monte Carlo estimation results*

It is of basic interest to achieve consistent estimation in finite samples of the first three components of β, i.e. the seasonal forcing r_t^*, the mixing parameter α_1 and ζ. We study their estimates for increasing order of approximation of the influx process.

Figure 2 summarizes the results for OLS and WLS estimation obtained for the zero-order model i.e. $c_i = 0$, $i = 1, 2, 3$. Each panel contains three graphs plotting the estimated r_t^*, ζ and α_1 against the six different population sizes on the log scale. The 26 seasonal parameters in r_t^* are summarized by their mean. Figure 2 illustrates that the variation of the estimates generally decreases with increasing population size. This is because the model variance in (13) is smaller for a large number of past infecteds. The other reason is that the effective sample size diminishes as smaller communities experience longer extinction times. The WLS estimator generally achieves a considerably lower variation of the estimates although the gain in efficiency is not substantial for the largest communities where the error distribution appears to be approximately Gaussian.

Considering the consistency of the estimates in finite samples the main message of Figure 2 is that, although the influx of infection may be approximately ignored for large cities, the parameter estimates are biased for the small and intermediate population sizes. This is especially obvious for the seasonal coefficients and the mixing parameter α_1.

Figure 3 shows that the bias may be reduced by increasing the degree of approximation of the influx process. The estimates are obtained by WLS. The first- and second-order approximations do not entail any obvious bias reduction. An order of one generally yields too large a value for α_1 and too small a

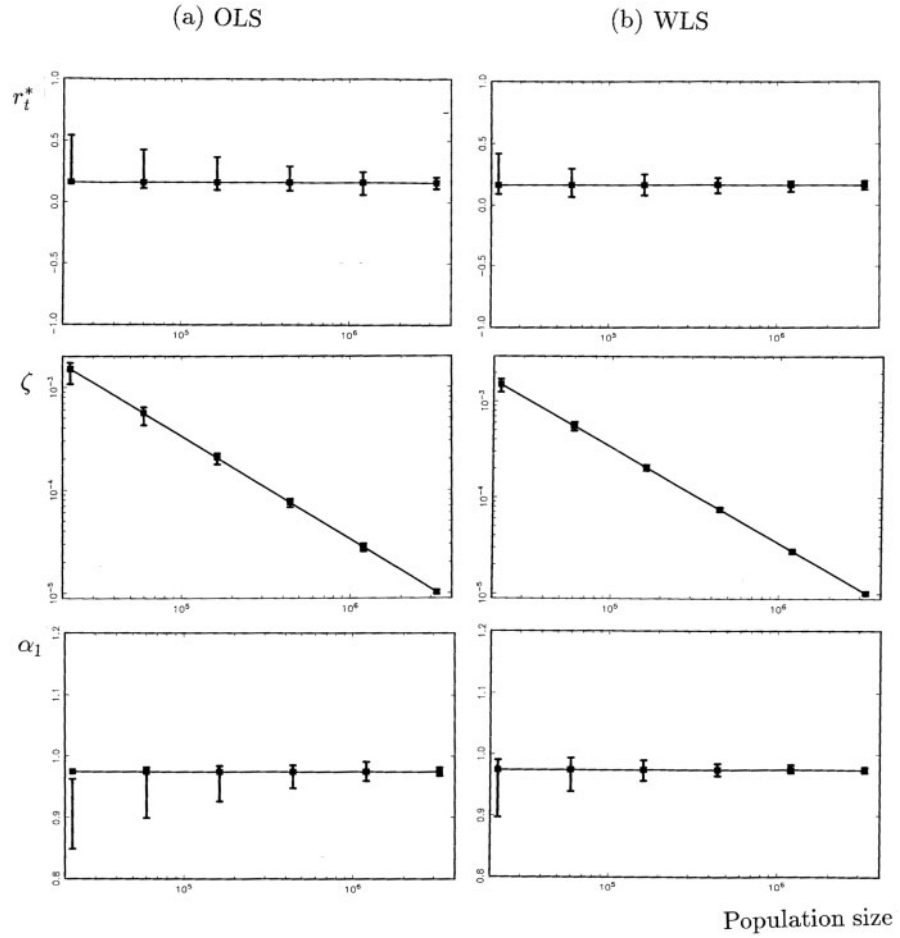

Fig. 2. Monte Carlo estimates (100 repetitions) of parameters against community size (log scale) for (a) ordinary least squares estimation and (b) weighted least squares estimation. The estimation model assumes $c_1 = c_2 = c_3 = 0$ (zero order). The vertical bars show the mean and the range of 1.96 times the empirical standard deviation around the mean for the 100 repetitions. The solid line connects the true parameter values. Results are plotted for (a) r_t^* (log scale, average over 26 seasonals), (b) ζ (log scale), and (c) α_1.

transmission parameter for the smaller cities. An order of two reduces the bias only slightly whereas an approximation of order three achieves seemingly consistent estimates even for the smallest city size in the sample. This is bought at the price of a larger variation of the estimates.

Interestingly, if the regression techniques are tested on simulated data from the stochastic model with deterministic influx rate $\theta_t = \theta$, then an approximation of an order as low as one achieves unbiased estimation with very small variation for any city size. We therefore presume that the need for a higher-order approximation is due to the influx being a stochastic variable.

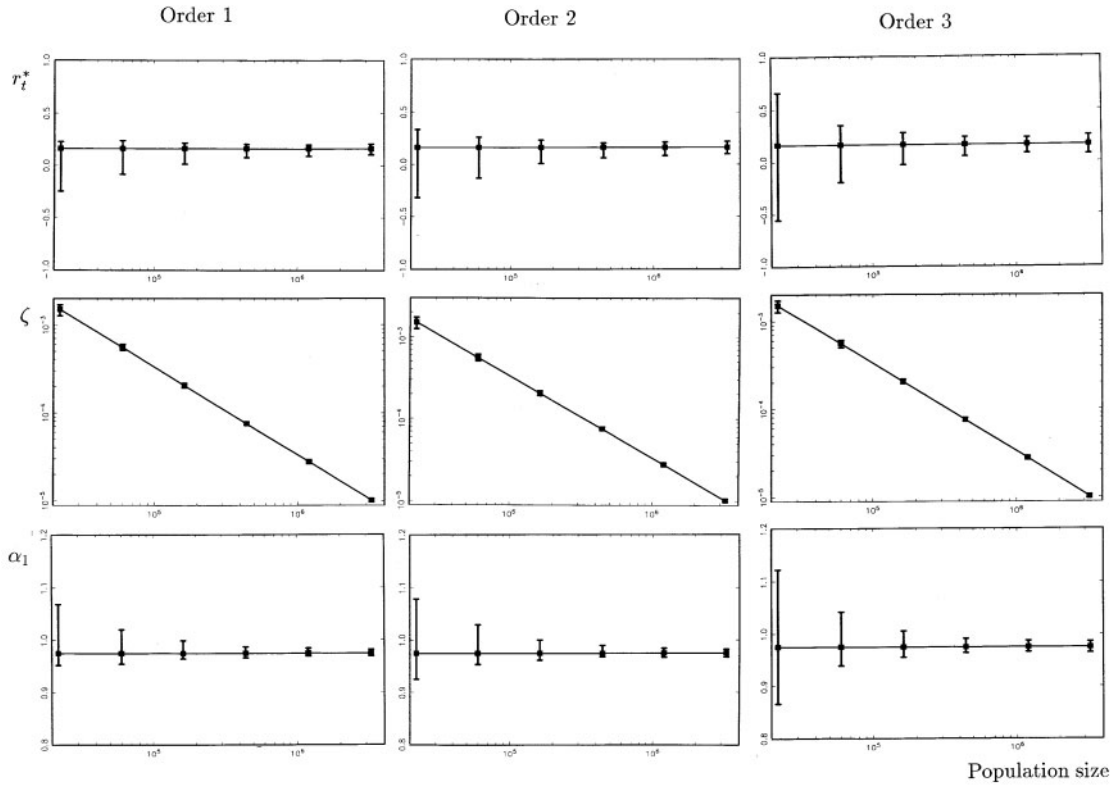

Fig. 3. Monte Carlo results for WLS estimators (100 repetitions) against community size. The parameters and the range of the vertical bars are as described in the previous figure. The order of the approximation is 1 in column 1, 2 in column 2, and 3 in column 3.

6. APPLICATION TO MEASLES DATA

Figure 4 summarizes the results of WLS estimation applied to the time series data from 60 cities. The estimates for the parameters $\log r_t^*, \zeta, \alpha_1$ are plotted against the corresponding population sizes where the seasonal coefficients are summarized by their yearly mean. The graphs also show the regression lines summarizing the parameter estimates for the 60 cities as functions of the populations sizes.

The effective sample size decreases from $T = 572$, i.e. the largest communities such as London, Birmingham and Liverpool never faded out, to $T = 162$ for the smallest community Teignmouth where the disease faded out for 70% of the time. The variation of the parameter estimates generally decreases with growing population size.

The estimates for $\log r_t^*$ (Figure 4(a)) do not vary systematically with population size. This can be expected as the population scaling of the original transmission rate r_t is balanced by the standardization with $\bar{S}$ that appears to be proportional to the population size. The average value for all 60 cities is 0.162 on the log scale which corresponds to an average transmission rate of 1.18 infecteds per time step if one infected is introduced into a host population with $\bar{S}$ susceptibles.

Figure 4(b) shows that the estimates for ζ scale negatively with population size. This can be expected as $\zeta = \alpha_2/\bar{S}$ is inversely proportional to the mean susceptible density. We can approximate the overall

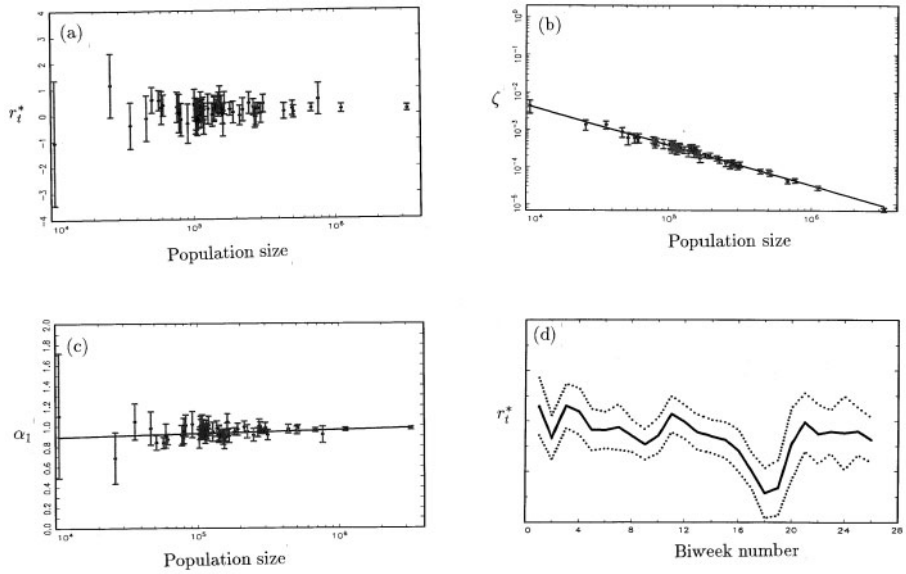

Fig. 4. Parameter estimates for 60 cities in England and Wales plotted against population size (log scale). The vertical bars show the parameter estimate plus/minus 2 times the estimated standard deviation obtained from the weighted least squares regression. (a) $\log r^*_{t \bmod s}$ (average over 26 seasonals) (b) ζ (log scale) with regression line as given in 17, (c) α_1 with regression line given in (18), (d) seasonal forcing: Seasonal coefficients $\log r^*_{t \bmod s}$ (average over 60 cities) against t mod s. The dotted lines show the 2 x (average) standard deviation band of the seasonal coefficients.

relationship between ζ and the population size by the regression

$$\log(\zeta) = 4.497 - 1.074 \log(\text{population size}) \tag{17}$$

where the standard errors are 0.204 and 0.017 for the intercept and the slope of the weighted regression, respectively.

The estimates of α_1 in Figure 4(c) appear to be slightly smaller than one (the weighted average is 0.958). This difference is significant for the four largest cities and for the majority of the remaining cities but, as variation of the estimates grows larger, it is not significant for some of the smaller and intermediate sized communities. Overall, this suggests the presence of an—albeit small—saturation effect. That is, for a fixed level of S_t, the number of infecteds in $t + 1$ is less than proportional to the number of infecteds in t. These results are in line with the estimate of $\alpha_1 = 0.968$ for the aggregate England and Wales data analysed in Finkenstädt & Grenfell (2000). Simulation studies of the stochastic model where we imposed $\alpha_1 = 1$ indicate that the dynamics are characterized by unrealistically large outbreaks followed by extinction even for community sizes well above the CCS. We presume that, for $\alpha_1 \geqslant 1$, the host population is depleted faster than it is replenished by births so that after a major outbreak the disease is forced to go extinct due to a lack of hosts. The saturation effect that is occurring for $\alpha_1 < 1$ decelerates the epidemics as a small proportion of susceptibles is rescued from infection. Together with the new recruitments from births, these provide an ongoing source of hosts so that the chain of transmission may be continued for a longer time after major epidemics. To summarize the estimates for the 60 cities we approximate the relationship between α_1 and the population size by

$$\alpha_1 = 0.749 + 0.0155 \log(\text{population size}) \tag{18}$$

where the coefficients are obtained from a weighted linear regression. The standard errors are 0.041 and 0.003 for the intercept and the regression slope, respectively.

Finally, Figure 4(d) shows the average (over 60 cities) seasonal pattern of $\log r_t^*$. The prominent dips in the annual variation of the transmission parameter coincide closely with the summer, Easter and Christmas school holidays. The average pattern of the seasonality in Figure 4(d) is almost identical to the pattern estimated for the aggregate England and Wales data in Finkenstädt & Grenfell (2000). A detailed discussion of the seasonal pattern is provided in Fine & Clarkson (1982) and Finkenstädt & Grenfell (2000).

The individual model fits for the 60 cities are remarkably good. The R^2 of the weighted regressions is only poor for the two smallest communities (Teignmouth 0.29, Kings Lynn 0.77), but otherwise achieves a level higher than 0.97 for more than half of the communities (0.996 for London).

7. INFERENCE ON THE INFLUX RATE

In principle, θ could be extracted from the coefficient of the linear expansion term. However, results from the Monte Carlo study suggest that its variation is of considerable magnitude if the Taylor expansion is of high order. We explore the use of a different approach based on the dynamics of the epidemics in simulations from the stochastic model.

The influx process θ_t plays a fundamental role in determining the epidemic dynamics for cities below the CCS. If there was no influx at all, the disease would remain extinct after an epidemic outbreak. If the influx is very small, the dynamics are characterized by long extinction times sporadically interrupted by massive outbreaks. On the other extreme, a very large influx rate leads to frequent outbreaks of low magnitude and very few or no extinctions. This suggests that there exists a 'realistic' range of θ such that the model behaviour is compatible with the epidemic dynamics observed in the time series data.

We quantify this by estimating the distances between the marginal density of the observed time series of infecteds and the marginal density of time series generated from the stochastic model for different influx rates. The model is conditioned on the observed local birth rates and based on the parameters from the population size as specified in the unified model in (18) and (17) with average seasonal forcing.

Let $\{X_t\}_{t=1}^n$ denote the observed time series of infecteds (including zero counts). Let $Y_t(\theta) = \{Y_t|\theta\}_{t=1}^n$ denote a realization from the stochastic model at mean influx rate θ and let θ vary over a grid $(0, \theta^{\max})$. Then

$$\hat{f}(x) = \frac{1}{n}\sum_{t=1}^{n} \frac{1}{h_n} k\left(\frac{x - X_t}{h_n}\right) \quad \text{and} \quad \hat{g}^{\theta}(x) = \frac{1}{n}\sum_{t=1}^{n} \frac{1}{h_n} k\left(\frac{x - Y_t(\theta)}{h_n}\right)$$

are estimated marginal densities of the observed time series and the stochastic simulation, respectively. Here, k is a Gaussian kernel function and h_n is the cross-validatory bandwidth (Silverman, 1986) obtained for the marginal density of the observed series. To estimate the distance between the densities we use the Kullback–Leibler-related measure (Skaug & Tjøstheim, 1996)

$$KL(\theta) = \frac{1}{n}\sum_{t=1}^{n} \log\left(\frac{\hat{f}(x_t)}{\hat{g}^{\theta}(x_t)}\right). \tag{19}$$

Figure 5 shows plots of $\log KL(\theta)$ against $\log\theta$, referred to as a KL plot for short, for some selected cities. We summarize the variation in the distance estimates by a local linear regression using a Gaussian kernel with a cross-validatory bandwidth. The KL plots possess a unique minimum around $\log\theta = -3$ for most UK cities, which corresponds to an average influx of one infected per 10 months. However, the pattern of the KL plot changes with population size. Small populations display a sharp minimum in their

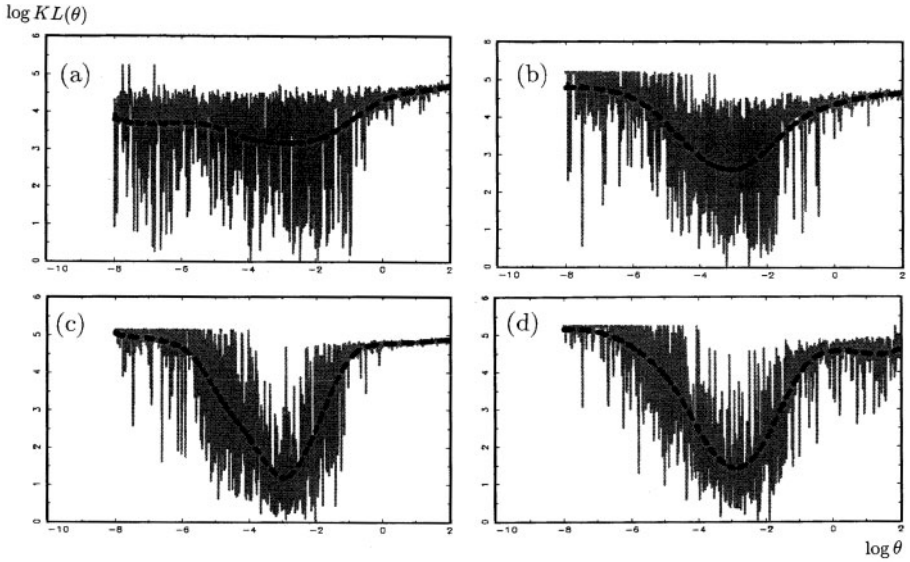

Fig. 5. Plot of the estimated distance $\log KL(\theta)$ against $\log\theta$ (KL plots) for a selection of cities: (a) Birmingham (1.1 million inhabitants), (b) Bristol (430 000 inhabitants), (c) Cambridge (93 000 inhabitants), (d) Exeter (77 000 inhabitants). Each point in the plot is the estimated KL distance for one realization of the epidemic model with a migration of $\log\theta$ where $\log\theta$ is varied over a grid of 1000 values in the range $[-8, 2]$.

KL plot. These become wider and less pronounced for increasing population size. For the largest cities, the KL plots are constant over a large range suggesting that the dynamics of the epidemics are not affected by variations in θ. Figure 6 shows the ranges of influx rates θ that minimize the estimated KL distances for each population size. The upper and lower boundaries correspond to an estimated $2\times$ local standard deviation band of the KL plots around their minimum. The lower bound is decreasing with population size suggesting that, in order for the epidemics to recur at the observed frequencies, larger cities need less influx than small cities. This is because, for increasing population size, there is a higher number of local infecteds and susceptibles that maintain the transmission chain for a longer time so that less influx from other areas is needed to spark off an epidemic. The upper bound of θ in Figure 6 is increasing with population size. The reason for this is that the effect of an increasing influx eventually becomes negligible in comparison with the size of a local epidemic if the host population is large anyway. The results in Figure 6 highlight the fact that our proposed estimator measures the influx rate on the basis of its importance relative to the local size of the host population. Whilst the dynamic pattern of the smallest city is compatible with a very small range of influx rates between 0.07 and 0.18 infecteds per biweek, endemic places such as London naturally do not respond to changes in influx over a much larger range. Moreover, this is what characterizes endemic communities.

8. Discussion

The main objective of our study is to provide a time series model for case notifications of childhood diseases in both large and small human host populations. Our work here extends upon a previous modelling approach by Finkenstädt & Grenfell (2000) which shows that the dynamical behaviour of measles in large human host populations can be captured remarkably well by a discrete-time continuous-

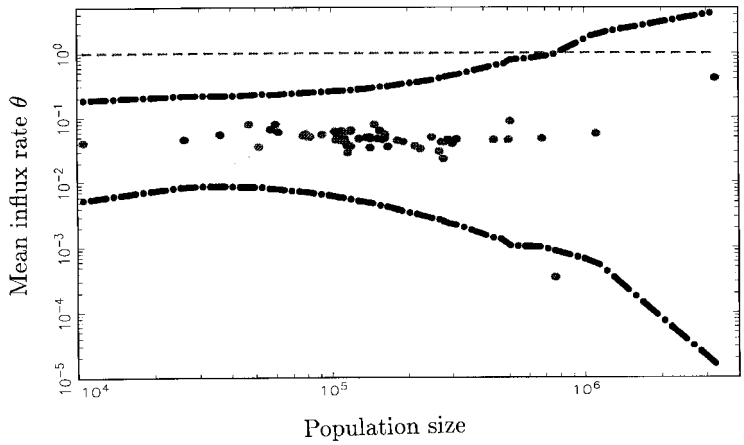

Fig. 6. Estimated influx θ (minimum of the smooth through the KL plots) plotted against the population sizes of the 60 cities. The two dot-dashed curves illustrate how the minima in the various KL plots become wider for growing population size. They are computed as follows. For each point in the KL plot we obtained an estimate of the local standard deviation from the kernel regression and computed another smooth through the set of points that denote the KL smooth minus 2 times the local standard error. This serves as our lower bound to the KL smooth. Then we computed the range of values of θ for which this lower bound is lower than or equal to the KL smooth evaluated at the minimum. This gives a range of values for θ for which the estimated KL distance is not 'significantly' different to the minimal KL distance. The two dot-dashed curves above are a smooth through these points. The dashed line denotes an influx of one infected per biweek.

valued model derived from epidemic theory. However, for small populations, the fluctuations arising from the stochastic structure of the epidemic process (process noise) are particularly important, as the number of infectives may become so small that the continuous-valued approximation is no longer valid. This necessitates the use of a discrete-valued stochastic model as developed here. Furthermore, the intrinsic noise due to the dispersal of infecteds has a crucial impact on the dynamics of the epidemics in small populations. This type of stochastic fluctuation is involved in the long-term dynamics of the epidemic process. We make use of this property in order to infer upon the mean rate of spatial influx.

Furthermore, we estimate model parameters from observed time series counts on measles for various different sizes of the host population. Here, we develop a regression approach and assess performance of estimation in a Monte Carlo study. The spatio-temporal data set for 60 cities can be seen as a replication of the epidemic process at different levels of community size and birth rate. It is therefore possible to study the scaling of the epidemic parameters as a function of the population size. The scaling uncovered here suggests that the parameter estimates can be unified by a single model. Moreover, since the seasonal schooling pattern is a common factor within the UK, it is possible to simulate the long-term dynamics for any given population size and birth rate on the basis of the common model. Figure 7 illustrates that realizations from this model capture the transition between type I, II and III dynamics for different sizes of the human host population.

The results obtained here serve as a starting point for more complicated estimation approaches based on Markov chain Monte Carlo algorithms which we are currently developing. Whilst in this study we have separated the susceptible dynamics from the transmission equation, an MCMC approach allows us to derive posterior distributions for all model parameters and states simultaneously. Developing such an algorithm is computationally sophisticated and expensive due to the fact that the epidemic model is

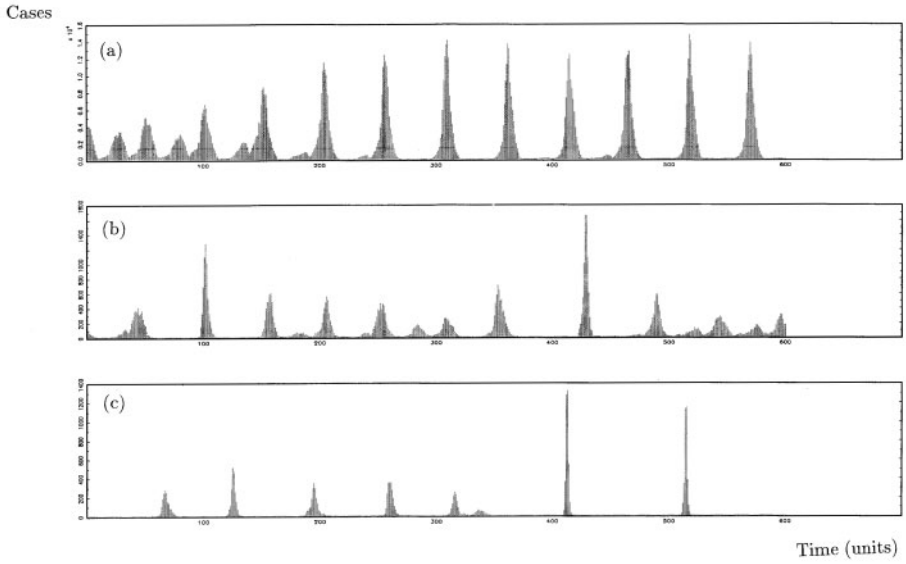

Fig. 7. Simulation examples from stochastic model with predicted parameters from population sizes (a) 3 million, (b) 150 000, (c) 50 000 inhabitants. The birth rate was set as 17 per thousand inhabitants per year and the mean influx rate as $\theta = \exp(-3)$.

nonlinear and incorporates different stochastic processes such as the measurement process, the migration process and the epidemic process itself.

We uncover an interesting dynamical tension between the local and the regional determinants of the dynamics. Spatial diffusion of infecteds between places is very important following local extinction (see also Finkenstädt & Grenfell (1998)) provided that the local pool of susceptibles has had time to be replenished. Intruigingly, the importance of migration becomes negligible as the disease spreads through the local chain of transmission. It is therefore only possible to reconstruct the rates of influx to the extent that influx was effectively necessary to produce the observed epidemic dynamics in the data. Even with the simple stochastic model used here one can perform a useful analysis of colonization and immigration of a disease in a community. An immigration of an infected from a different community will not always spark off an epidemic in a population where measles has faded out. The chance of sparking off an epidemic depends on the transmission rates of the disease and size of the susceptible population replenished by births. Bjørnstad *et al.* (2002) study the odds of sparking off an epidemic given one immigrant and show how the influence of any additional immigrant is decreasing. This explains further why there is so little information pertaining to the migration process in large cities.

The results of this study give rise to a host of other epidemiological questions to be addressed in future research. We briefly point out some of them here.

Ecologists have for a long time viewed power laws or non-mass-action terms such as these to be the signature of spatial processes (Hassel & Varley, 1969; Lui *et al.*, 1987). Our results do not confirm the mass action assumption. Simulation studies, not reported here, indicate that the saturation effect that occurs for $\alpha_1 < 1$ seems to have a profound impact on the epidemic dynamics and the time to extinction. It is therefore interesting to study whether the saturation effect gives more realistic predictions of Bartlett's critical community size than a mass action model. Also, further studies are necessary that compare the interpretation of epidemic parameters in continuous-time dynamical models with the discrete-time

approximations used to fit the time series of measurements (Glass and Grenfell, in preparation).

The stochastic model suggested here adds another ingredient to the longstanding discussion about the predictability of measles time series (Schaffer & Kot, 1985; Olsen & Schaffer, 1990; Sugihara *et al.*, 1990; Ellner, 1991; Nychka *et al.*, 1992; Grenfell, 1992; Tidd *et al.*, 1993). Since, for cities below the CCS, the onset and therefore the timing of epidemic outbreaks after extinction is determined by the stochastic influx, the predictability of epidemics hinges on the influx process. Thus, the predictability of recurrent epidemics must decrease with community size to the same extent that extinction becomes more frequent and spatial influx rather than local infection becomes the major catalyst of epidemics. The question of measles' predictability with respect to periodicity and city size is studied in further detail in Grenfell *et al.* (2002) where the empirical power spectra of the observed time series are compared with the power spectra of TSIR model simulations and local Lyapunov exponents are derived for endemic populations. Our next aim is to extend these results to understand the more important applied problem of predictability of measles and other childhood infections in the vaccine era.

Finally, the decrease in predictability for small population size would be less drastic if our assumption about the influx process were modified to allow for a more realistic but also more complex spatial coupling. Time series simulations from the stochastic model exhibit a certain level of synchrony for different cities which is due to the common seasonality. However, this is generally not as high as the observed spatial synchrony between neighbouring cities in England and Wales. This indicates that there is extra correlation due to spatial epidemic coupling of close communities. It is possible to implement a more explicit spatial coupling mechanism into the stochastic model by assuming that θ is a function of the epidemic states in neighbouring communities. We address such model extensions in future research.

ACKNOWLEDGEMENTS

This research was supported by the Wellcome Trust (BFF and BTG), the National Center for Ecological Analysis and Synthesis (ONB) and the Norwegian Science Foundation (ONB). The authors wish to thank two anonymous referees for suggestions that have improved the presentation.

REFERENCES

ANDERSON, R. M. AND MAY, R. M. (1991). *Infectious Diseases of Humans: Dynamics and Control*. Oxford: Oxford University Press.

BARTLETT, M. S. (1956). Deterministic and Stochastic Models for Recurrent Epidemics. *Proceedings of the Third Berkeley Symposium on Mathematical Statistics and Probability* **4**, 81–108.

BARTLETT, M. S. (1957). Measles Periodicity and Community Size. *Journal of the Royal Statistical Society,* Series A **120**, 48–70.

BARTLETT, M. S. (1960a). The Critical Community Size for Measles in the US. *Journal of the Royal Statistical Society,* Series A **123**, 37–44.

BARTLETT, M. S. (1960b). *Stochastic Population Models in Ecology and Epidemiology*. London: Methuen.

BJØRNSTAD, O. N., FINKENSTÄDT, B. F. AND GRENFELL, B. T. (2002). Endemic and epidemic dynamics of measles. I. Estimating transmission rates and their scaling using a time series SIR model. *Ecological Monographs* in press.

BLACK, F. L. (1984). Measles. Evans, A. S. (ed.), *Viral Infections of Humans: Epidemiology and Control*. New York: Plenum, pp. 397–418.

BOBASHEV, G. V., ELLNER, S. P., NYCHKA, D. W. AND GRENFELL, B. T. (1998). Reconstructing susceptible and recruitment dynamics from measles epidemic data. *Mathematical Population Sciences.* In press.

DIETZ, K (1975). Transmission and Control of Arbovirus Diseases. In Ludwig, D. and Cooke, K. L. (eds), *Epidemiology*, Philadelphia: SIAM, pp. 104–121.

DIETZ, K. (1976). The Incidence of Infectious Diseases under the Influence of Seasonal Fluctuations. *Lecture Notes in Biomathematics* **11**, 1–15.

ELLNER, S. P. (1991). Detecting Low-Dimensional Chaos in Population Dynamics Data: a Critical Review. In Logan, J. and Hain, F. (eds), *Chaos and Insect Ecology*, Charlottesville: University Press of Virginia, pp. 63–90.

ELLNER, S. P. AND TURCHIN, P. (1995). Chaos in a Noisy World: New Methods and Evidence from Time Series Analysis. *American Naturalist* **145**, 343–375.

ELLNER, S. P., BAILEY, B. A., BOBASHEV, G. V., GALLANT, A. R., GRENFELL, B. T. AND NYCHKA, D. W. (1998). Noise and Nonlinearity in Measles Epidemics: Combining Mechanistic and Statistical Approaches to Population Modeling. *American Naturalist* **151**, 425–440.

FINE, P. E. M. AND CLARKSON, J. A. (1982). Measles in England and Wales I: An Analysis of Factors underlying Seasonal Patterns. *International Journal of Epidemiology* **11**, 5–14.

FINKENSTÄDT, B. F. AND GRENFELL, B. T. (1998). Empirical Determinants of Measles Metapopulation Dynamics in England and Wales. *Proceedings of the Royal Society*, Series B **265**, 211–220.

FINKENSTÄDT, B. F. AND GRENFELL, B. T. (2000). Time Series Modelling of Childhood Diseases: a Dynamical Systems Approach. *Applied Statistics* **49**, 187–205.

FINKENSTÄDT, B. F., KEELING, M. J. AND GRENFELL, B. T. (1998). Patterns of Density Dependence in Measles Dynamics. *Proceedings of the Royal Society*, Series B **265**, 753–762.

GRENFELL, B. T. AND, (1992). Chance and Chaos in Measles Dynamics. *Journal of the Royal Statistical Society*, Series B **54**, 383–398.

GRENFELL, B. T., BJØRNSTAD, O. N. AND FINKENSTÄDT, B. F. (2002). Endemic and epidemic dynamics of measles. II. Scaling noise, determinism and predictability with the time series SIR model. *Ecological Monographs* in press.

GRENFELL, B. T. AND BOLKER, B. M. (1998). Cities and villages: infection hierarchies in a measles metapopulation. *Ecology letters* **1**, 63–70.

GRENFELL, B. T. AND HARWOOD, J. (1997). (Meta)population dynamics of infectious diseases. *Trends in Ecology and Evolution* **12**, 395–399.

HARVEY, A. C. (1976). Estimating Regression Models with Multiplicative Heteroscedasticity. *Econometrica* **44**, 461–465.

HASSEL, M. P. AND VARLEY, G. C. (1969). A New Inductive Population Model for Insect Parasites and its Bearing on Biological Control. *Nature* **223**, 1133–1136.

KEELING, M. J. AND GRENFELL, B. T. (1997). Disease Extinction and Community Size: Modeling the Persistence of Measles. *Science* **275**, 65–67.

KENDALL, D. G. (1949). Stochastic Processes and Population Growth. *Journal of the Royal Statistical Society*, Series B **11**, 230–264.

KERMACK, W. O. AND MCKENDRICK, A. G. (1933). A Contribution to the Mathematical Theory of Epidemics. Part III. Further studies of the problem of endemicity. *Proceedings of the Royal Society*, Series A **141**, 92–122.

LONDON, W. P. AND YORKE, J. A. (1973). Recurrent Outbreaks of Measles, Chickenpox and Mumps. I. Seasonal Variation in Contact Rates. *American Journal of Epidemiology* **98**, 453–68.

LUI, W. M., HETHCOTE, H. W. AND LEVIN, S. A. (1987). Dynamical Behaviour of Epidemiological Models with Nonlinear Incidence Rates. *Journal of Mathematical Biology* **25**, 359–380.

MCCULLAGH, P. AND NELDER, J. A. (1997). *Generalized Linear Models. Second edition*. Boca Raton: Chapman and Hall/CRC.

NYCHKA, D., ELLNER, S., GALLANT, A. R. AND MCCAFFREY, D. (1992). Finding Chaos in Noisy Systems. *Journal of the Royal Statistical Society,* Series B **54**, 399–426.

OLSEN, L. F. AND SCHAFFER, W. M. (1990). Chaos Versus Noisy Periodicity: Alternative Hypotheses for Childhood Epidemics. *Science* **249**, 499–504.

RHODES, C. J., JENSEN, H. J. AND ANDERSON, R. M. (1997). On the Critical Behaviour of Simple Epidemics. *Proceedings of the Royal Society,* Series B **264**, 1639–1646.

SCHAFFER, W. M. AND KOT, M. (1985). Nearly One Dimensional Dynamics in an Epidemic. *Journal of Theoretical Biology* **112**, 403–427.

SCHENZLE, D. (1984). An Age-Structured Model of Pre- and Post-Vaccination Measles Transmission. *IMA Journal of Mathematics Applied in Medicine and Biology* **1**, 169–191.

SCHWARTZ, I. B. (1985). Multiple Recurrent Outbreaks and Predictability in Seasonally forced nonlinear Epidemic Models. *Journal of Mathematical Biology* **18**, 233–253.

SILVERMAN, B. W. (1986). *Density Estimation for Statistics and Data Analysis*. London: Chapman and Hall.

SKAUG, H. J. AND TJØSTHEIM, D. (1996). Measures of Distance between Densities with Application to Testing Serial Independence. In Robinson, P. M. and Rosenblatt, M. (eds), *Time Series Analysis in Memory of E. J. Hannan*, New York: Springer, pp. 363–377.

SOPER, M. A. (1929). The Interpretation of Periodicity in Disease Prevalence. *Journal of the Royal Statistical Society,* Series A **92**, 34–61.

SUGIHARA, G., GRENFELL, B. T. AND MAY, R. M. (1990). Distinguishing Error from Chaos in Ecological Time Series. *Philosophical Transactions of the Royal Society,* Series B **330**, 235–251.

TIDD, C. W., OLSEN, L. F. AND SCHAFFER, W. M. (1993). The Case for Chaos in Childhood Epidemics: II. Predicting Historical Epidemics from Mathematical Models. *Proceedings of the Royal Society,* Series B **254**, 257–73.

YORKE, J. A. AND LONDON, W. P. (1973). Recurrent Outbreaks of Measles, Chickenpox and Mumps; Systematic Differences in Contact Rates and Stochastic Effects. *American Journal of Epidemiology* **98**, 469–482.

[*Received April 30, 2001; first revision October 1, 2001; second revision November 1, 2001; accepted for publication November 13, 2001*]